J Mater Sci (2011) 46:1259–1263
DOI 10.1007/s10853-010-4908-3

Synthesis and luminescence properties of a novel Eu^{3+}, Tb^{3+} co-doped $Al_{18}B_4O_{33}$ whiskers by a gel nano-coating method

Jian Wang · Guiling Ning · Weitao Gong · Junwei Ye · Yuan Lin

Received: 26 July 2010 / Accepted: 6 September 2010 / Published online: 23 September 2010

Abstract $Al_{18}B_4O_{33}$:Eu^{3+}, Tb^{3+} whiskers have been successfully prepared by a simple gel nano-coating method using aluminum isopropoxide as the starting materials. X-ray diffraction (XRD), scanning electron microscopy (SEM), transmission electron microscopy (TEM), high-resolution transmission electron microscopy (HRTEM), selected area electron diffraction (SAED), photoluminescence (PL), and thermogravimetric analysis (TGA) were used characterize the samples. The results show coexistence of the crystal phase $Al_{18}B_4O_{33}$, amorphous phase, and Eu^{3+}, Tb^{3+} ions of the samples with initial addition Al/B ratios from 3 to 1 are incorporated into the amorphous phase. The $Al_{18}B_4O_{33}$:Eu^{3+}, Tb^{3+} whiskers are very straight with an average diameter of 600 nm and lengths ranging from 5 to 10 μm. Under ultraviolet excitation at 365 nm, samples show mainly exhibit the characteristic emission of Eu^{3+} corresponding to $^5D_0 \rightarrow F_{1,2}$ transitions due to an efficient energy transfer occurs from Tb^{3+} to Eu^{3+}.

Introduction

Rare-earth-activated inorganic phosphor materials have been widely used in modern lighting and display fields, such as fluorescent lamps, cathode-ray tubes, field emission displays for their well-defined transitions within the 4*f* electronic shells [1–5]. As the most frequently used activator ions in luminescent materials, the Eu^{3+} and Tb^{3+} are excellent activator which mainly show emissions due to transitions of $^5D_0$ to ^7F_J ($J = 1, 2, 3, 4$) in the red region and $^5D_4$ to ^7F_J ($J = 6, 5, 4, 3$) in the green region, respectively [6, 7]. Moreover, it is well-known that an effective energy transfer can take place from Tb^{3+} to Eu^{3+} in several hosts [8–10].

Borates have been proved to be useful in optical materials because of their high stability, low synthesis temperature, and their high ultraviolet (UV) transparency and nonlinear properties [11]. Aluminum borate ($Al_{18}B_4O_{33}$) is a promising ceramic materials in this family for excellent mechanical properties, chemical inertness, low thermal expansion coefficient, and high-temperature stability [12–15]. In previous study, $Al_{18}B_4O_{33}$ containing rare earth elements (Ce^{3+}, Tb^{3+}, Eu^{3+}) have been reported [16–18]. However, so far little attention has been paid to synthesis and luminescent properties of Eu^{3+} and Tb^{3+} co-doped $Al_{18}B_4O_{33}$ and the corresponding energy transfer from Tb^{3+} to Eu^{3+} in $Al_{18}B_4O_{33}$ glass–ceramic composites has not been realized and reported. On the other hand, luminescence of amorphous materials was paid little attention. This is due to the fact that the quantum yield of an amorphous material is not so high as those of a well-defined crystalline family. However, glasses are well-known in optically pumped laser materials containing Nd^{3+} [19].

Accordingly in this article, we report the synthesis of $Al_{18}B_4O_{33}$:Eu^{3+}, Tb^{3+} crystalline-amorphous material by nano-coating method. Comparing with the previous reports [16–18], our present study is very different. We added boric acid to the aluminum isopropoxide alcohol solution to ensure boric acid and aluminum isopropoxide in the

J. Wang (✉)
School of Chemical Engineering, University of Science and Technology LiaoNing, High-Tech District 185 Qianshan Middle Road, Anshan 114051, People's Republic of China
e-mail: anshantonywang@yahoo.com.cn

G. Ning · W. Gong · J. Ye · Y. Lin
State Key Laboratory of Fine Chemicals and School of Chemical Engineering, Dalian University of Technology, 158 Zhongshan Road, Dalian 116012, People's Republic of China

isopropyl alcohol react completely. Subsequently, the Al^{3+} in aluminum isopropoxide combines with boric acid during Lewis acid–base reaction to give amorphous aluminum borate. When the deionized water was added to the mixture dropwise, the remnants of aluminum isopropylate which undergo hydrolysis and polycondensation reactions can be utilized to coat a stable layer of alumina on amorphous aluminum borate containing of Eu^{3+} and Tb^{3+}. After calcinating at higher temperatures, the glass–ceramic $Al_{18}B_4O_{33}$:Eu^{3+}, Tb^{3+} phase is thus obtained. The gel nano-coating method enhances mechanical properties and structural stability of the glass–ceramic $Al_{18}B_4O_{33}$:Eu^{3+}, Tb^{3+} and makes rare earth elements uniformly disperse in the final product. Moreover, we investigated the energy transfer property from Tb^{3+} to Eu^{3+} in $Al_{18}B_4O_{33}$ crystalline-amorphous material.

Experimental

Sample preparation

The starting materials include the following chemicals: H_3BO_3 (99.9%), Eu_2O_3 (99.99%), Tb_2O_3 (99.99%), and aluminum isopropoxide (99.99%). Aluminum isopropoxide was synthesized from high-purity aluminum metal and isopropanol, and then purified by a followed controlled distillation process [20]. The detailed synthesis procedures were described as follows: Tb_2O_3, Eu_2O_3 (molar ratio Eu/(Al + B) = 0.01, Tb/(Al + B) = 0.01) and 0.05 mol aluminum isopropoxide were premixed in 50 mL isopropanol solvent under stirring, followed by the addition of different molar H_3BO_3. The deionized water was added to the vigorously stirred mixture dropwise until aluminum isopropoxide hydrolyzed completely, and then formed a gel precursor. It was dried at 60 °C for 4 h and further calcined for 3 h at 1,250 °C in an alumina crucible.

Characterization

The as-synthesized samples were examined by XRD measurement on a Rigaku-DMax 2400 diffractometer equipped with graphite monochromatized CuKα ($\lambda = 1.5406$ Å). Infrared spectroscopy (IR) was measured on a JASCO460 plus spectrophotometer. The excitation and emission spectra were recorded on a JASCO FP-6300 spectrofluorometer. The morphology of the samples was characterized by scanning electron microscopy (SEM, JSM-5600LV, JEOL). The TEM observation was carried out using a Philips TECNAI G^2 s-twin microscope. The formation of the different crystalline phrases was analyzed by TGA. Thermal analyses were carried out at 10 °C min^{-1} under air atmosphere on Mettler Toledo apparatuses (TG/DTA 815^e).

Results and discussion

XRD patterns of the samples with initial addition Al/B molar ratio varying from 4.5:1 to 1:1 are shown in Fig. 1. The pattern of the samples with initial addition Al/B = 4.5:1 shows that there are strong diffraction peaks of $Al_{18}B_4O_{33}$ phase (JCPDS 32-0003) along with weak diffraction peaks of Al_2O_3 (JCPDS 1-1307), $EuBO_3$ (JCPDS 13-0485) and $TbBO_3$ (JCPDS 24-1272). Both $EuBO_3$ and $TbBO_3$ exhibit very similar X-ray diffraction patterns with hexagonal-vaterite structure. This result indicates that as-synthesized samples are a mixture of $Al_{18}B_4O_{33}$, Al_2O_3, $EuBO_3$, and $TbBO_3$, in which Eu^{3+} and Tb^{3+} ions have not build into the $Al_{18}B_4O_{33}$ host lattice without change of its surroundings.

As the initial addition Al/B molar ratio from 3:1 to 1:1, the diffraction peaks of Al_2O_3, $EuBO_3$, and $TbBO_3$ crystalline phases disappear. Only the crystal phase of $Al_{18}B_4O_{33}$ is observed. This result indicates that a great change of Eu^{3+} and Tb^{3+} surroundings occurs with an increase of H_3BO_3 concentration.

From the XRD results mentioned above, it seems impossible that Eu^{3+} and Tb^{3+} ions are incorporated into the crystal lattice of $Al_{18}B_4O_{33}$, because Eu^{3+} and Tb^{3+} ions have a much larger radius, compared with Al^{3+} and B^{3+} ions.

Therefore, it can be inferred that the increase of H_3BO_3 concentration may give rise to an increase of amorphous phase, and Eu^{3+}, Tb^{3+} ions dope into amorphous phase. This finding is similar the previously result reported in [16].

SEM micrograph given in Fig. 2a, b shows the morphology of Eu^{3+} and Tb^{3+} co-doped $Al_{18}B_4O_{33}$ whiskers with initial addition molar ratio Al/B = 1:1. Large

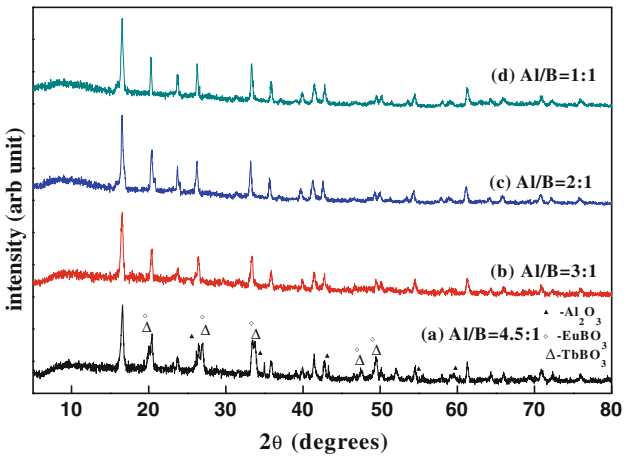

Fig. 1 XRD patterns of the Samples with different initial addition Al/B ratios: (*a*) 4.5:1, (*b*) 3:1, (*c*) 2:1, (*d*) 1:1. The *marks* indicate diffraction lines of (*filled triangle*) Al_2O_3 (*open diamond*) $EuBO_3$ (*open triangle*) $TbBO_3$

amounts of whiskers twist around one another to form a large aggregate (Fig. 2a). A closer examination of the samples indicates that the interweaving whiskers are very straight with an average diameter of 600 nm and lengths ranging from 5 to 10 μm.

The microscopic structure of Eu^{3+} and Tb^{3+} co-doped $Al_{18}B_4O_{33}$ whiskers with initial addition molar ratio Al/B = 1:1 is further characterized by the TEM technique accompanied by SAED. TEM observations (Fig. 3a) showed that there are two types of particles A and B. Particle A has thin film structure, while particle B shows thick structure. The selected area electron diffraction patterns taken from a white square were found to have diffraction points and diffuse rings. It is strongly suggested that amorphous phase and crystalline phase coexist in the samples and Eu^{3+} and Tb^{3+} are doped into the amorphous phase. It should be noted that there are weak diffraction rings in the amorphous particle A, indicating that a small of crystallites exist.

$Al_{18}B_4O_{33}$:Eu^{3+}, Tb^{3+} whiskers with initial addition molar ratio Al/B = 1:1 show a red–orange emission under UV excitation. Figure 4 shows the excitation and emission spectra of the sample. The excitation spectrum of samples monitored at 613 nm is composed of two excitation bands of Eu^{3+} and Tb^{3+}. The f–f transitions within Eu^{3+} $4f^6$ electron configuration (main peaks at the 365, 383, 396, 406, 468 nm) is corresponding to the electron transitions from the $^7F_0$ ground state to $^5D_4$, $^5L_7$, $^5L_6$, $^5D_3$, $^5D_2$), with $^5F_0 \rightarrow {}^5L_6$(396 nm) transition as most intense peak [21]. The characteristic f–f transition lines within the Tb^{3+} $4f^8$ configuration is assigned as the transitions from the $^7F_6$ ground state to the different excited states of Tb^{3+}, that is, 374 nm ($^5G_6$) 490 nm ($^5D_4$), respectively [22]. The emission spectrum of samples (Fig. 4b) under 365 nm excitation consists of four bands. Besides Eu^{3+} emissions, we can also observe the characteristic emissions of Tb^{3+}. The peaks at about 489, 541 nm are due to Tb^{3+} transitions from $^5D_4$ to ^7F_J ($J = 6, 5$), and the other emission peaks at about 591, 613 nm are from the $^5D_0$ to ^7F_J ($J = 1, 2$). Among these luminescence emission peaks, the emission spectrum is dominated by the hypersensitive red transition at 613 nm. The most prominent emission line at 613 nm is due to hypersensitive electronic dipole transition of $^5D_0 \rightarrow {}^2F_7$, induced by the lack of inversion symmetry at Eu^{3+} local sites, while the emission near 591 nm is the magnetic dipole transition owing to the $^5D_0 \rightarrow {}^7F_1$ states, which obey the selection rule ($\Delta j = 0, \pm 1$), and its intensity hardly varies with evolution of the surroundings [18].

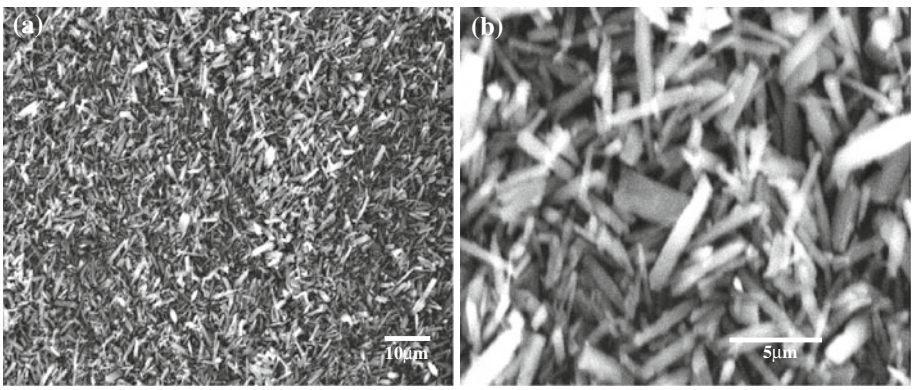

Fig. 2 SEM images of the Samples with Al/B = 1:1 **a** high-density $Al_{18}B_4O_{33}$:Eu^{3+}, Tb^{3+} whiskers twisted together; **b** magnified image of $Al_{18}B_4O_{33}$:Eu^{3+}, Tb^{3+} whiskers

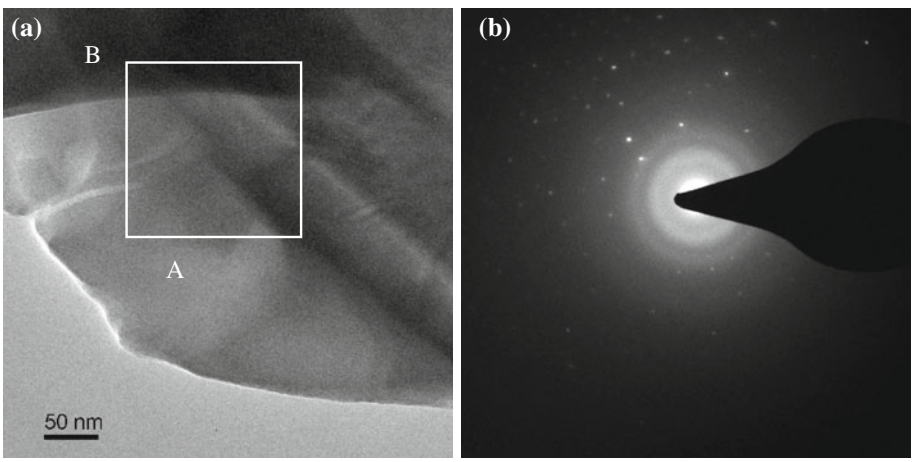

Fig. 3 **a** HRTEM image of $Al_{18}B_4O_{33}$:Eu^{3+}, Tb^{3+} whiskers. **b** Selected area diffraction image taken from a *white square* (*inset* **a**)

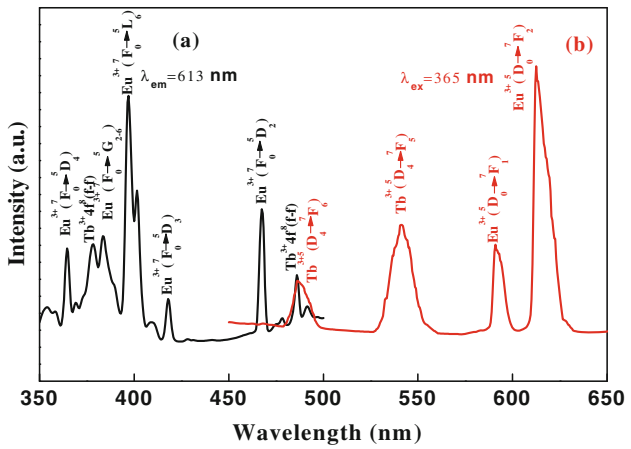

Fig. 4 Excitation (*a*) and emission (*b*) spectra of the $Al_{18}B_4O_{33}:Eu^{3+}$, Tb^{3+} whiskers with initial addition Al/B ratios 1:1

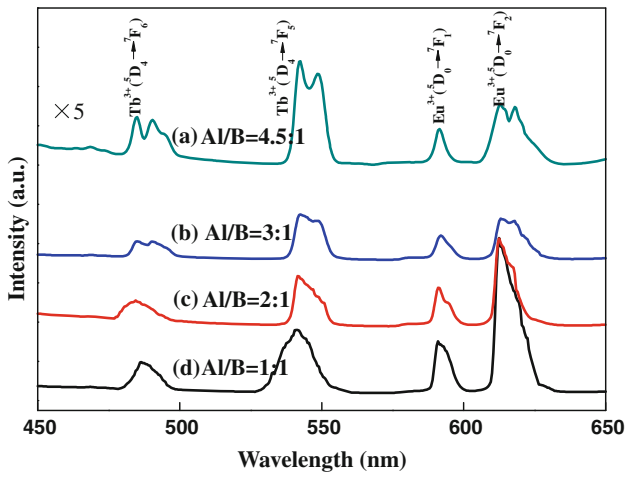

Fig. 5 Emission spectra of the $Al_{18}B_4O_{33}:Eu^{3+}$, Tb^{3+} samples with different initial addition Al/B ratios: (*a*) 4.5:1, (*b*) 3:1, (*c*) 2:1, (*d*) 1:1 under 365 nm excitation

Figure 5 shows the emission spectra of $Al_{18}B_4O_{33}:Eu^{3+}$, Tb^{3+} with initial addition Al/B varying from 4.5 to 1 under 365 nm excitation. With the increase of H_3BO_3 concentration, the intensity of Eu^{3+} and Tb^{3+} emissions become stranger. Meanwhile, Eu^{3+} and Tb^{3+} emission lines become inhomogeneous and broadened. This characteristic feature of Eu^{3+} and Tb^{3+} emission spectra is quite similar to that of Eu^{3+} and Tb^{3+} in an amorphous has a characteristic features: inhomogeneous broadening of luminescence band [23]. When initial addition Al/B ratio changes from 4.5 to 1, this change of luminescent properties reveals a variation of Eu^{3+} and Tb^{3+} surroundings, indicating that Eu^{3+} and Tb^{3+} of the samples dope into an amorphous phase with the increase of H_3BO_3 quantity. Moreover, the emission from the $^5D_3$ level of Tb^{3+} has not been observed in this sample, which can be explained by the quenching of

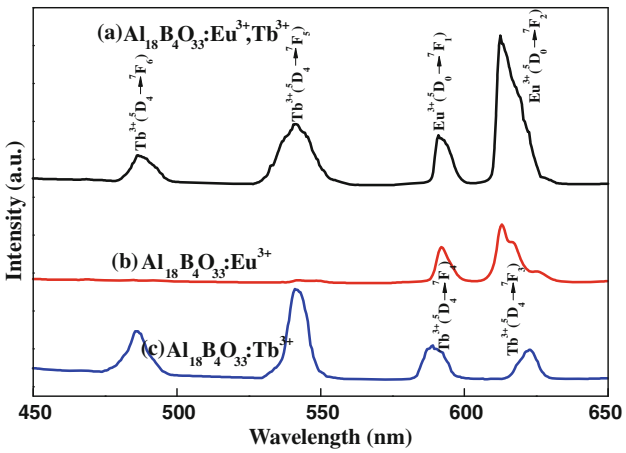

Fig. 6 Emission spectra of samples (*a*) $Al_{18}B_4O_{33}:Eu^{3+}$, Tb^{3+}, (*b*) $Al_{18}B_4O_{33}:Eu^{3+}$, (*c*) $Al_{18}B_4O_{33}:Tb^{3+}$

the efficient multiphonon de-excited with lattice vibration due to the high energy of phonons in the borates [17].

The emission spectrum of $Al_{18}B_4O_{33}:Eu^{3+}$, Tb^{3+}, $Al_{18}B_4O_{33}:Eu^{3+}$, and $Al_{18}B_4O_{33}:Tb^{3+}$ (initial addition molar ratio Al/B = 1:1) under 365 nm excitation are presented in Fig. 6 for comparison. In the $Al_{18}B_4O_{33}:Tb^{3+}$ samples, only the characteristic emissions of Tb^{3+} are observed. With the doping of Eu^{3+} and Tb^{3+} in the $Al_{18}B_4O_{33}$, besides Tb^{3+} emission, we can also observe the characteristic emissions of Eu^{3+}. With the addition Eu^{3+}, the luminescence of Tb^{3+} decrease (Fig. 6), and that of Eu^{3+} increases, both due to the enhancing the probability of energy transfer from Tb^{3+} to Eu^{3+}. All results above indicate an efficient energy transfer behavior shows that $Al_{18}B_4O_{33}:Eu^{3+}$, Tb^{3+} is not a mixture of $TbBO_3$ and $EuBO_3$, but aluminoborate glass phase, in which Eu^{3+} and Tb^{3+} has been incorporated the aluminoborate glass phase at certain H_3BO_3 concentration. Otherwise, the $Tb^{3+} \rightarrow Eu^{3+}$energy transfer can not occur in the separated phases [10]. A summary of emission and energy transfer process of Eu^{3+} and Tb^{3+} in $Al_{18}B_4O_{33}$ is described in below. First, electrons on Tb^{3+} ions are excited from the ground state ($4f^8$) to the excited state ($4f^75d$) by UV light. Subsequently, these electrons relax to the lowest excited state $^5D_4$ through multiphonon relaxation then either return to the ground state to produce the emissions ($^5D_4 \rightarrow {}^7F_{6,5,4,3}$) or transfer their excitation energy from $^5D_4$ (Tb^{3+}) level to the higher excited energy levels of Eu^{3+} ($4f^6$) through cross relaxation, which relax to the $^5D_0$ (Eu^{3+}) level, where the red–orange emission ($^5D_0 \rightarrow {}^7F_{0,1,2,3,4,5,6}$) takes place [24]. Because the $^5D_4 \rightarrow {}^7F_{6,5,4,3}$ emission of Tb^{3+} is effectively overlapped with the $^7F_{0,1} \rightarrow {}^5D_{0,1,2}$ absorption of Eu^{3+}, the energy transfer from Tb^{3+} to Eu^{3+} is very efficient in general.

Figure 7 represents the TGA analysis of amorphous aluminum borate containing of Eu^{3+} and Tb^{3+}. The TGA

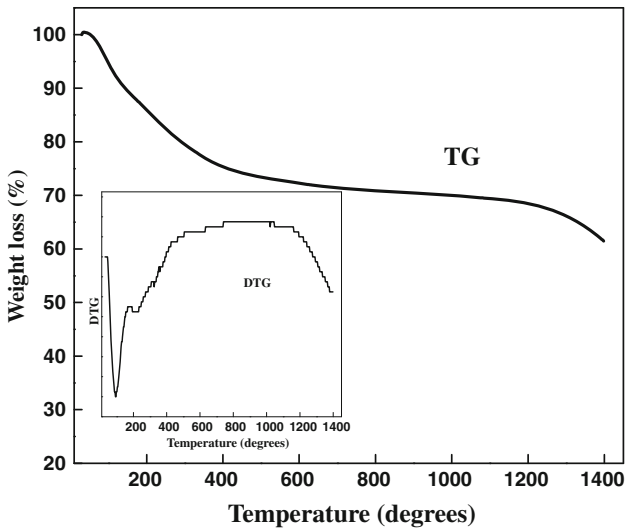

Fig. 7 Thermogravimetry and differentiate thermogravimetry trace of the as-synthesized $Al_{18}B_4O_{33}$:Eu^{3+}, Tb^{3+} samples

curves present two stages of weight loss and the total weight loss of about 31.5%. The initial weight loss between 30 and 210 °C results from desorption of isopropoxide alcohol and boric acid from the surface of amorphous precursors. During this process, H_3BO_3 will decompose into B_2O_3 at about 185 °C, and then B_2O_3 will melt at about 430 °C. There is no structural change till 750 °C. It is assigned to the glass–ceramic $Al_4B_2O_9$:Eu^{3+}, Tb^{3+} without any weight variation. The weight loss was detected at around 1,150–1,400 °C, which corresponds to melting of $Al_4B_2O_9$ phase and a yield of $Al_{18}B_4O_{33}$ and liquid [25].

Conclusion

In summary, we have demonstrated that a simple and mild gel nano-coating method for synthesis of the glass–ceramic $Al_{18}B_4O_{33}$:Eu^{3+}, Tb^{3+} whiskers. The results reveal coexistence of the crystal phase $Al_{18}B_4O_{33}$ and aluminoborate glass phase and Eu^{3+}, Tb^{3+} ions are incorporated into the aluminoborate glass phase at certain H_3BO_3 concentration. $Al_{18}B_4O_{33}$:Eu^{3+}, Tb^{3+} exhibits a red–orange emission spectrum, consisting of four emission bands peaking at 489, 541, 591, and 613 nm. With initial addition Al/B molar ratio change from 4.5 to 1, Eu^{3+} and Tb^{3+} emission intensity increase. An efficient energy transfer can occur from Tb^{3+} to Eu^{3+} in the glass–ceramic $Al_{18}B_4O_{33}$:Eu^{3+}, Tb^{3+} whiskers, which are ascribed to the energy overlap between Eu^{3+} and Tb^{3+}. Further study is under way to modify luminescent color by controlling the doping concentration of Eu^{3+} and Tb^{3+} ions, for different composition of emissions of Eu^{3+} and Tb^{3+} resulted from energy efficiency at different doping concentration of Eu^{3+} and Tb^{3+}.

Acknowledgements The authors gratefully acknowledge support of National Natural Science Foundation of China (No. 20772014), National High Technology Research and Development Program of China (863 Program) (No. 2008AA03A325) and Young Teachers' Training Fund of Dalian University of Technology (No. 893377).

References

1. Yu M, Lin J, Fu J, Zhang HJ (2003) J Mater Chem 13:1413
2. Capobianco JA, Vetrone F, Boyer JC, Speghini A, Bettinelli M (2002) Opt Mater 19:259
3. Evans RC, Carlos LD, Douglas P, Rocha J (2008) J Mater Chem 18:1100
4. Dotsenko VP, Berezovskaya IV, Efryushina NP (2010) J Mater Sci 45:1469. doi:10.1007/s10853-009-4104-5
5. Shan ZF, Chen DQ, Yu YL, Huang P, Lin H, Wang YS (2010) J Mater Sci 45:2775. doi:10.1007/s10853-010-4266-1
6. Blasse G, Grabmaier BC (1994) Luminescent materials. Springer-Verlag, Berlin
7. Silva ACS, Souza GG, Nobre MAL (2010) J Mater Sci 45:4216. doi:10.1007/s10853-010-4516-2
8. Holloway WW, Kestigian M, Newman R (1963) Phys Rev Lett 11:458
9. Chen W, Sammynaiken R, Huang Y (2000) J Appl Phys 88:1424
10. Di WH, Wang XJ, Zhu PF, Chen BJ (2007) J Solid State Chem 180:467
11. Wang YH, Li XX (2006) J Electrochem Soc 153:238
12. Suganuma K, Fujita T, Suzuki N, Niihara K (1990) J Mater Sci Lett 9:633
13. Ma R, Bando Y, Sato T, Tang C, Xu F (2002) J Am Chem Soc 124:10668
14. Ma R, Bando Y, Sato T (2002) Appl Phys Lett 81:3467
15. Liu Y, Li Q, Fan S (2003) Chem Phys. Lett 375:632
16. You HP, Hong GY (1999) J Phys Chem Solids 60:325
17. You HP, Hong GY, Wu XY (2003) Chem Mater 15:2000
18. Elssfah E, Tang CC (2007) J Phys Chem C 111:8176
19. Thomas LM, Stephen AP, Gary DW (1992) J Non-Cryst Solids 151:183
20. Ning GL, Lin Y, Lv BL (1997) J Dalian Univ Technol 37:269
21. Balda R, Fernádez J, Adam JL, Arriandiaga MA (1996) Phys Rev B 54:12076
22. Thomas KS, Singh S, Dieke GH (1963) J Chem Phys 38:2180
23. Tanabe S, Hirao K, Soga T, Hanada T (1992) J Solid State Chem 97:481
24. Nakazawa E, Shionoya S (1967) J Chem Phys 47:3211
25. Gielisse PJM, Foster WR (1962) Nature 69:195